J|A|C|S COMMUNICATIONS

Published on Web 03/06/2009

Self-Assembly of Nanostructured Diatom Microshells into Patterned Arrays Assisted by Polyelectrolyte Multilayer Deposition and Inkjet Printing

Wei Wang,[†] Timothy Gutu,[‡] Debra K. Gale,[†] Jun Jiao,[‡] Gregory L. Rorrer,[†] and Chih-hung Chang*[,†]

Department of Chemical Engineering, Oregon State University, Corvallis, Oregon 97331, and Department of Physics, Portland State University, Portland, Oregon 97201

Received November 19, 2008; E-mail: changch@engr.orst.edu

In nature, a few classes of organisms have the ability to fabricate inorganic materials into complex hierarchical patterns by bottom-up self-assembly processes.[1] For example, diatoms are a prolific class of single-celled algae that possess microscopic, biogenic silica shells or "frustules" with intricate nanoscale features, including two-dimensional pore arrays.[2] Recently, it has been shown that intact diatom frustules possess blue photoluminescence,[3] act as 2D photonic crystals,[4,5] and can be biologically functionalized with antibodies.[6] These properties enable device applications such as optical platforms for gas sensors,[7] electroluminescent thin films with novel emission patterns,[8] and biosensing.[9] Scalable processes for assembling these biologically fabricated microstructures into defined patterns are needed in order to take advantage of their nanoscale features and properties for future device applications in optoelectronics and bionanotechnology.

The layer-by-layer deposition method developed by Decher's group[10,11] is a powerful technique in which the ionic interaction between surface charges manipulates the adsorption of a polyelectrolyte onto a surface. Although this method by itself does not enable patterning, it does serve as a vehicle for selective assembly when used in combination with other patterning techniques.[11−14] For example, charged silica colloidal particles can be selectively deposited on oppositely charged polyelectrolyte multilayers (PEMs) formed by a layer-by-layer process patterned through microcontact printing.[12]

Herein, we report the self-assembly of a rectangular array of single-diatom frustules onto a glass surface. The fabrication process was mediated by the selective adsorption of the diatom biosilica onto a PEM-patterned surface through inkjet printing. Positively charged poly(allylamine hydrochloride) (PAH, 15 000 g/mol) and negatively charged poly(sodium 4-stryrene sulfonate) (PSS, 70 000 g/mol) served as the polyelectrolyte pair for the PEM.

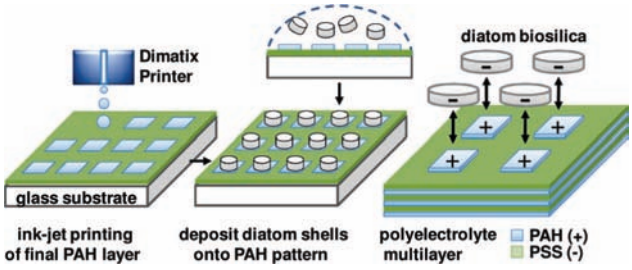

Figure 1. Schematic illustration of the fabrication process.

A schematic illustration of the process is shown in Figure 1. Glass has a negative surface potential due to exposed silanol (SiOH) groups.[10] Positively charged PAH was first deposited onto cleaned glass slides by dipping, followed by a rinsing and drying step using high-purity water and flowing N_2. A second layer of negatively charged PSS was then adsorbed on top of the first PAH layer, followed by another rinsing and drying step. Usually, eight polyelectrolyte layers (four PAH/PSS bilayers) were successively formed, resulting in a negatively charged top layer. The measured ζ potentials for sucessive PAH and PSS layers were 20 and −20 mV, respectively, which are close to the reference values for these materials.[15] The average thickess of each layer was 8.6 nm, and spreading was not controlled.

A final patterned layer of positively charged PAH was printed onto the underlying surface layer of negatively charged PSS using a Dimatix printer. Figure 2 presents epifluorescence microscope images of a representative PAH pattern. To visualize the printed layer, the dye rhodamine-123 (R-123, CAS registry no. 62669-70-9, Sigma-Aldrich R8004) was added to the PAH ink. The R-123 tracer revealed the shape of the printed dot and also showed that the highest concentration of the ink was near the center of the dot. The actual diameters of the dots were ∼300−350 μm, as shown in Figure 2a, although the desired size was 150 μm. Spreading of the dot was caused by the wetting of the PAH ink on the PEM. The measured contact angle for the PAH ink on the PEM (20°) was lower than that for pure water because of the hydrophobicity of both the PAH ink and the underlying polyelectrolyte layer. The bright centers were from absorption of R-123 onto NaCl crystals in the PAH ink.

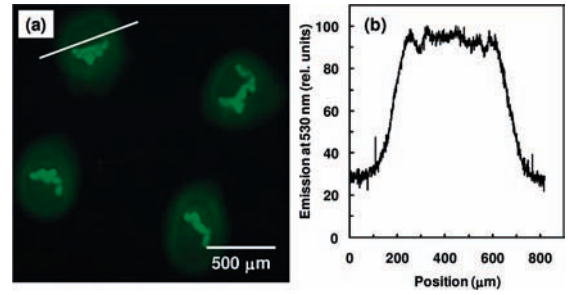

Figure 2. Visualization of the printed PAH pattern on the $(PAH/PSS)_4$ PEM: (a) epifluorescence microscope image at 530 nm emission; (b) line scan of the image intensity.

Intact biosilica frustules of the large centric diatom *Coscinodiscus wailesii* (∼200 μm) and the small centric diatom *Cyclotella* sp. (∼10 μm) were isolated by hydrogen peroxide treatment of cultured cells using methods described previously.[16] In order to image the frustules by light microscopy, *Coscinodiscus* cells were incubated in Harrison's nutrient medium[17] containing 5.0 μM of R-123,[18] which was metabolically incorporated into the biosilica of the new frustule formed after cell division. This process labeled 80% of the total frustules with R-123 after the 7 day cultivation period. An aqueous suspension of the diatom frustules was pipetted directly

[†] Oregon State University.
[‡] Portland State University.

10.1021/ja809079n CCC: $40.75

onto the PAH-printed PEM (Figure 1). The film was mixed gently on an orbital shaker to disperse the suspension. The biosilica-adsorbed PEM was then rinsed with high-purity water. Since the biosilica surface of the diatom frustule possesses silanol groups,[3] they were attracted only to the printed PAH area and not to the exposed PSS area. The diameter of *Coscinodiscus* was nominally the same as the printed PAH dot. Consequently, only one disk-shaped diatom frustule was deposited onto a given PAH dot. By this method, a rectangular array of individual diatom frustules was formed. Figure 3a shows a representative 2 × 2 portion of the

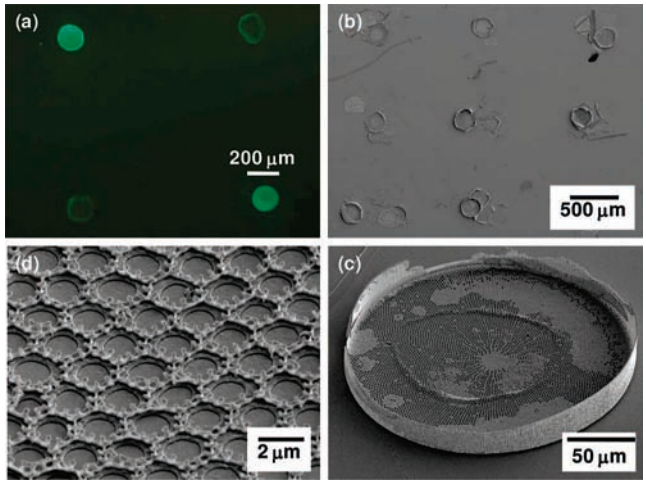

Figure 3. Epifluorescent and SEM images of *Coscinodiscus* frustules deposited on a PAH-printed PEM: (a) 2 × 2 array of R-123-labeled diatom frustules imaged by epifluorescence at 530 nm; (b) 3 × 3 array of single *Coscinodiscus* frustules imaged by SEM; (c) SEM image of a single *Coscinodiscus* diatom frustule, inside surface facing up; (d) SEM image of fine features of the pore array on the diatom biosilica surface, with the PAH-printed PEM surface underneath.

printed array of *Coscinodiscus* frustules labeled with R-123. The difference in dye intensity reflected the variation in the extent of dye incorporation into the frustule biosilica during cell-wall biosynthesis. Figure 3b−d shows scanning electron microscopy (SEM) images of the self-assembled *Coscinodiscus* diatom frustule array on the printed PEM. The inkjet printing process provided order at the microscale, whereas the diatom surface itself provided order and 3D topology at the submicron and nanoscales.

We also patterned the small centric diatom *Cyclotella* using the same techniques, as shown in Figure 4. Several hundred of the 10

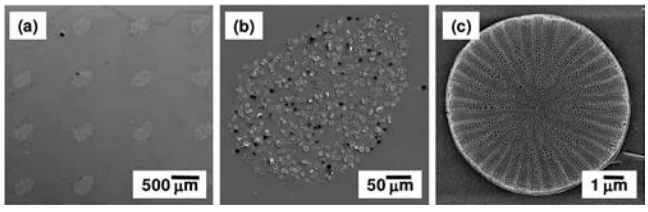

Figure 4. SEM images of *Cyclotella* diatom frustules deposited on PAH-printed PEM dots: (a) 4 × 4 array of printed PAH dots, each containing a single layer of frustules; (b) Single layer of frustules on a single PAH dot; (c) fine features of a single frustule on the PAH dot.

μm *Cyclotella* frustules were closely deposited as a monolayer that conformed to the elliptical shape of the printed PAH dot. Each individual frustule had ordered fine features at the nanoscale. The adsorbed diatoms adhered to the substrate after vigorous washing by water and methanol.

We have identified several key parameters that control the adsorption of diatom frustules. PAH is a weak polyelectrolyte with the ionic equilibrium reaction $[RNH_3^+]_n + OH^- \rightleftarrows [RNH_2]_n + H_2O$, where R is dedicated to the carbon chain and n is the degree of polymerization. When the pH goes above 8.5 (the pK_a value of PAH[19]), the OH^- ions in the solution react with H^+ groups on the backbone of PAH, resulting in lower biosilica adsorption. The influence of pH on the adsorption density is shown in the Supporting Information (see Figure S3). Adjusting the ionic strength in solution is another way to control the adsorption of biosilica. The addition of NaCl assists the development of polyelectrolyte layers via charge screening and provides extrinsic charge compensation.[19] In this context, the frustule biosilca only adsorbed to the printed PAH layer when NaCl was added to the solution, which was verified by experiment. Furthermore, since the glass surface was not perfectly smooth, there had to be enough polyelectrolyte layers to suppress the influence of the substrate. By experiment, a minimum of eight layers was required.

In conclusion, individual shells of the diatom *Coscinodiscus* self-assembled into a rectangular array on a glass surface that possessed a polyelectrolyte multilayer patterned through inkjet printing. This patterned thin film possessed hierarchical order with nanostructure provided by the diatom biosilica. The process used two polyelectrolytes with opposite electric potentials to control the surface charge of the substrate. In comparison with microcontact printing, where a specific stamp has to be fabricated before printing, inkjet printing offers a no-contact, maskless patterning process. Furthermore, the fine features of the diatom frustules were perfectly preserved as a result of the mild conditions of the deposition process. This technique has the potential to enable large-scale device applications that harness the unique properties of functionalized diatom biosilica.

Acknowledgment. This research was supported by the National Science Foundation (NSF) under Nanoscale Interdisciplinary Research Team Award BES-0400648.

Supporting Information Available: Procedures for all of the experiments. This material is available free of charge via the Internet at http://pubs.acs.org.

References

(1) Mann, S.; Ozin, G. A. *Nature* **1996**, *382*, 313.
(2) Sumper, M.; Brunner, E. *Adv. Funct. Mater.* **2006**, *16*, 17–26.
(3) Qin, T.; Gutu, T.; Jiao, J.; Chang, C.-H.; Rorrer, G. L. *J. Nanosci. Nanotechnol.* **2008**, *8*, 2392.
(4) Yamanaka, S.; Yano, R.; Hisanao, U.; Hayashida, N.; Ohguchi, M.; Takeda, H.; Yoshino, K. *J. Appl. Phys.* **2008**, *103*, 074701.
(5) De Stefano, L.; Rea, I.; Rendina, I.; De Stefano, M.; Moretti, L. *Opt. Express* **2007**, *15*, 18082.
(6) Townley, H. E.; Parker, A. R.; White-Cooper, H. *Adv. Funct. Mater.* **2008**, *18*, 369.
(7) Lettieri, S.; Setaro, A.; De Stefano, L.; De Stefano, M.; Maddalena, P. *Adv. Funct. Mater.* **2008**, *18*, 1257–1264.
(8) Jeffryes, C.; Solanki, R.; Rangineni, Y.; Wang, W.; Chang, C.-H.; Rorrer, G. L. *Adv. Mater.* **2008**, *20*, 2633.
(9) De Stefano, L.; Rotiroti, L.; De Stefano, M.; Lamberti, A.; Lettieri, S.; Setaro, A.; Maddalena, P. *Biosens. Bioelectron.* [Online early access]. DOI: 10.1016/j.bios.2008.08.016. Published Online: Aug 20, 2008. Gale, D. K.; Gutu, T.; Jiao, J.; Chang, C.-H.; Rorrer, G. L. *Adv. Funct. Mater.* [Online early access]. DOI: 10.1002/adfm.200801137. Published Online: Feb 9, 2009.
(10) Decher, G. *Science* **1997**, *277*, 1232.
(11) Decher, G. *Multilayer Thin Films*; Wiley-VCH: Weinheim, Germany, 2003; pp 1−30.
(12) Chen, K. M.; Jiang, X.; Kimerling, L. C.; Hammond, P. T. *Langmuir* **2000**, *16*, 7825.
(13) Lyles, B. F.; Terrot, M. S.; Hammond, P. T.; Gast, A. P. *Langmuir* **2004**, *20*, 3028.
(14) Caruso, F.; Susha, A. S.; Giersig, M.; Möhwald, H. *Adv. Mater.* **1999**, *11*, 950.
(15) Ladam, G.; Schaad, P.; Voegel, J. C.; Schaaf, P.; Decher, G.; Cuishinier, F. *Langmuir* **2000**, *16*, 1249.
(16) Jeffryes, C.; Gutu, T.; Jiao, J.; Rorrer, G. L. *Mater. Sci. Eng., C* **2008**, *28*, 107.
(17) Harrison, P. J.; Waters, R. E.; Taylor, F. J. R. *J. Phycol.* **1980**, *16*, 28.
(18) Brzezinski, M. A.; Conley, D. J. *J. Phycol.* **1994**, *30*, 45.
(19) Burke, S. E.; Barrett, C. J. *Langmuir* **2003**, *19*, 3297.

JA809079N